

Research journal articles as document genres: exploring their role in knowledge organization

V Kalyani, S. Leelashyam, M Venkataratnam

Associate Professor, Assistant Professor

Department of ECE,

vkalyani.ece@anurag.ac.in, vleelashyam.ece@anurag.ac.in, mvenkataratnam.ece@anurag.ac.in

Anurag Engineering College, Kodada, Telangana

Abstract

Deep learning is one of the most promising machine learning techniques that revolutionized the artificial intelligence field. The known traditional and convolutional neural networks (CNNs) have been utilized in medical pattern recognition applications that depend on deep learning concepts. This is attributed to the importance of anomaly detection (AD) in automatic diagnosis systems. In this paper, the AD is performed on medical electroencephalography (EEG) signal spectrograms and medical corneal images for Internet of medical things (IoMT) systems. Deep learning based on the CNN models is employed for this task with training and testing phases. Each input image passes through a series of convolution layers with different kernel filters. For the classification task, pooling and fully-connected layers are utilized. Computer simulation experiments reveal the success and superiority of the proposed models for automated medical diagnosis in IoMT systems.

KEYWORDS

AI, anomaly detection (AD), corneal images, deep learning, EEG signals, IoMT, machinelearning, traditional CNNs

INTRODUCTION

In medical applications that depend on medical signal and image processing, automatic diagnosis is considered a basic task. The principle of automatic medical diagnosis is built on the anomalous behavior in signals or images to be detected. Anomaly detection (AD) can be implemented on medical images such as eye images or on medical signals such as electroencephalography (EEG) signals. In this paper, we will investigate the AD problem with both medical images and signals with deep learning tools. Both corneal images and EEG signals are considered in this study.

The human eye is a delicate extension of the brain that is encased and protected by the skull bones. There are three layers of the eye. The cornea is the translucent, front portion of the outer layer through which light passes. The fragile receptors inside the eye are protected by the remaining outer layer of the eye, which is made up of a white sclera. The choroid is the second or intermediate layer. It also contains blood arteries that provide the eye with nutrition. The retina specialized receptor cells are found in the innermost layer.

The cornea is the dome-shaped structure in the anterior part. The cornea provides the eye with two-thirds of its focusing or refractive capacity. The remaining third is created by the internal crystal lens. It is essential that the anterior part of the eyeball, the cornea, remains moist. This is achieved by the eyelids, which, upon awakening, sweep away the lacrimal glands and other surface secretions at regular intervals, while sleeping covers the eyes and protects them.

The EEG signals need to be analyzed for epileptic activity detection. For epilepsy patients, EEG signals are composed of normal, pre-ictal and ictal activities. The behavior of EEG signals reflects the epilepsy patient status.¹ The EEG seizure detection task depends on the detection of ictal activities, while the EEG seizure prediction task depends on the detection of the pre-ictal activities.

There are several examples for implementing the automatic medical diagnosis based on medical inspection with signal and image processing tools. The techniques of AD can be utilized for determining the exudates and microaneurysms in the images of the optical fundus.² The main challenge in this interesting area is designing an efficient system for detecting and capturing abnormal activities for automatic medical diagnosis from medical signals or images with high efficiency.³ The traditional convolution neural networks (CNNs) have been considered the common deep learning tools used for solving the problems of image classification. In this research paper, a CNN is utilized for

detecting anomalies based on medical image processing concepts. The CNN contains several layers. It consists of convolutional, pooling, dropout, and fully-connected (FC) layers. The filters within the convolutional layer (CNV) perform the 2D convolution on the input images, and the pooling layers (PLs) decrease the feature map size.^{3,4}

Epileptic seizures are known as the transient and unexpected electrical disturbances of the brain. At least, one out of 100 persons experiences a seizure. Unfortunately, the epileptic seizure mechanism is not fully understood. In addition, its occurrence is unpredictable. The EEG signal contains information about brain activities. It can be used for clinical brain activity check. Within the EEG signal, the epileptic form discharge detection can be considered a critical step in the epilepsy diagnosis. The traditional method of epilepsy detection based on visual inspection of EEG recordings is inefficient, and it consumes a long time. Therefore, the EEG signal can be used to diagnose the medical status of the human brain by extracting the parameters of the EEG signal. Hence, automatic medical diagnosis for brain diseases can be performed based on intelligent parameter extraction from the EEG signals of the brain.⁵

In this study, proposed models are presented for processing of corneal images and EEG signals for allowing automatic medical diagnosis. In this technique, the original version of the EEG signal is transformed into an image by using the spectrogram estimation, and the spectrogram is used directly as an input to the CNN. The proposed technique has been tested and evaluated on the scalp CHB-MIT database for three patients. It works as a detection tool for normal versus ictal, and normal versus pre-ictal activities. Besides, it classifies the three cases of the EEG signal, which are normal, ictal and pre-ictal. The obtained simulation results prove the ability of the proposed automatic diagnosis technique to detect and classify the status of the human brain based on EEG signals.

The contributions of this paper can be illustrated as follows:

1. Discussing the problem of medical signal and image diagnosis by considering EEG signals and corneal images.
2. Building a deep learning model for automatic diagnosis of corneal image abnormalities.
3. Handling the EEG signals and transforming them into suitable forms to be used as inputs for deep learning models.
4. Building an automatic detection and prediction system of EEG signal abnormalities for epilepsy seizure problems.

The rest of this paper is structured as follows. In Section 2, the related work is presented. The proposed automatic diagnosis techniques are discussed in Section 3. Section 4 is devoted to the specifications of the used datasets. Section 5 presents the simulation experiments and results. The conclusions are presented in Section 6.

RELATED WORK

This paper is concerned with the problem of AD from both biomedical signals and images. This study covers AD from EEG signals and corneal images. In this section, a literature review related to the discussed issues is included.

Related work to corneal image processing

The outer eye tunic consists of the cornea and sclera. It prevents objects from passing to the eye and acts as a protective shield for the eye. There are five main layers in the cornea, which are epithelium layer, Bowman's layer, stroma layer, Descemet's membrane, and endothelium layer. Each layer has a specific role that helps in the mechanical operation of the eye. For example, the stroma layer leftover water flows out via endothelium layer. The cornea inner layer is the corneal endothelium. It is very important in diagnosing the cornea status. Hexagonal cells make up the majority of the cells in the inner layer. Their shape and structure are used to provide important medical information regarding the cornea health. The fifth layer is the corneal endothelium layer. It is a monolayer cell, and it affects the human vision.⁵

The effect of age on visual acuity is considered to be a major problem. The normal function of eye tissues decreases with age. Hence, intelligent computer systems can be used to classify different eye diseases. The computer-based tools can be very useful and effective in diagnosing diseases. There are several vision problems such as distortion, clouding, and blindness due to corneal diseases. Keratoconus, Fuchs' endothelial dystrophy, and bullous keratopathy are three kinds of corneal diseases. Keratoconus is a condition in which the center cornea weakens. Keratoconus is a condition that affects one or both eyes. The second corneal disease is Fuchs' endothelial dystrophy, which is a hereditary disorder of the cornea inner cell layer, and this is known as the endothelium. Bullous keratopathy is the third corneal disease. It is a disorder in which the cornea stays continuously swollen. This happens when the endothelium, the cornea inner

layer, is no longer able to pump fluids out of the tissue.⁶

Several researchers have discussed corneal diseases, such as Tang, Mohammed, and Girisha.⁴⁻⁶ They mentioned that corneal diseases cause clouding, distortion and blindness. The automatic diagnosis of eye diseases can be performed through medial inspection of eye images. There are various techniques and approaches that were presented in previous articles for corneal image processing such as enhancement, histogram processing, and segmentation of medical images. The results from this classification achieved an accuracy of 77% for guttation, 83% for Fuchs' dystrophy, 82% for posterior dystrophy, and 82% in the case of iridocorneal.

The image processing approach for corneal images has been proposed in different research papers such as Ayala, Sanchez, and Nadachi⁷⁻⁹ for improving the quality of corneal images. Several research works have been presented with proposed solutions to segment the endothelial images. A numerical assessment of corneal layers using wavelet analysis has been presented with the help of local grey-scale thresholds. Several researchers proposed different methods for determining the intensity of cell boundaries to calculate hexagonal cell density for achieving the automatic diagnosis.¹⁰⁻¹²

In 2006, Kannathal et al.¹³ presented three classifiers and presented a comparison between them for classifying the corneal images with an artificial neural network (ANN). All these classifiers have been trained on 80 images, containing 30 normal images and 50 abnormal images.¹³ Segmentation of corneal endothelial layer images has been proposed by Piorkowski et al.¹⁴ for the analysis of these images with directional filters. The automatic estimation of the corneal image cell density has been implemented in 2005 by Alfredo Ruggeri and Enrico Grisan, and in 2002 by Marco. The circular band of the discrete Fourier transform (DFT), which determines the endothelium layer spatial frequency, is extracted using the DFT based on cell density.^{15,16} In 2008, Gavet presented an algorithm based on the frequency-domain information to compute the corneal cell borders with the help of neural networks.¹⁷ In 2005, Grisan and Paviotti proposed a method for calculating the cell density of the endothelium layer. In addition, the properties of the endothelium cells have been investigated in this article. The cell contours are defined before estimating the cell density for classifying the corneal images.¹⁸⁻²⁰ An efficient automatic corneal image segmentation method has been presented in Fabijanska.²¹ It depends on the determination of pixel locations and cell boundaries to form what is called an edge map. A comparison between different state-of-the-art techniques is shown in Table 1.²¹⁻²⁴

| Related work to EEG signal processing

The problem of abnormality detection from EEG signals is considered in this paper. The main objective is epilepsy detection. The electrical activity disruption in the brain is known as a seizure. Epilepsy disease is a brain abnormality that causes a patient to have recurrent seizures.^{25,26} World Health Organization (WHO) reported that there are 50 million people, who suffer from epilepsy in the world. In addition, the number of active epilepsy cases that need treatment in the general population is 4–10 in every 1000 persons, while in other low-income countries, the numbers increase to 7–14 in every 1000 persons.²⁷

Really, EEG is a brain impulse recording. It is also known as the activity of the brain cell neurons across the scalp. A local current flow is produced when the neurons are activated. The EEG signal reflects these flows by the electrodes "flat metal discs."²⁸ EEG readings and parameter extraction are used to develop the concept of automatic seizure detection and prediction. This subject attracts several researchers to present efficient approaches for automatic seizure detection and prediction based on the utilization of EEG parameters in the EEG signal classification. Therefore, the feature extraction from EEG signals is the main process in an EEG signal classification system. This paper is mainly concerned with the utilization of a lower-complexity technique for feature extraction with the help of a CNN model for classification.

As known, the automatic diagnosis of different diseases such as epilepsy is an attractive and interesting research point. Different research works have presented different methods for this purpose. Dalton et al.²⁹ proposed a body sensor network for detecting seizures using time-domain analysis. This trend achieved a sensitivity of detection of 90%, and its specificity equals 84%. Other seizure detection strategies based on frequency-domain processing have been presented in several research works. Khamis et al.³⁰ proposed a frequency-domain signal representation for detecting seizures. Its sensitivity is 91%.

Shoeb et al.³¹ utilized the wavelet transform for extracting EEG signal features. This trend depends on wavelet decomposition for obtaining the feature vector of the EEG signal. Moreover, several researchers used the wavelet transform for the same purpose. A seizure detection approach based on wavelet and temporal characteristics was presented

by Meier et al.³² The wavelet transform is utilized with different classifiers such as the ANN based on cumulative thresholds for analyzing the EEG signals to introduce an efficient tool that can detect seizures, automatically.^{33,34} Shoeb and Guttag presented another machine-learning-based technique. It combines spectral and spatial EEG features with non-EEG features in one vector. This method depends on the SVM as a classifier.³⁴⁻³⁶

The seizure activity analysis is performed by extracting temporal features using cellular NNs. Moreover, bidirectional recurrent NNs have been recommended for EEG signal analysis by Vidyaratne et al.³³ Emami et al.³⁷ introduced a technique for EEG seizure detection through CNN-based analysis of scalp images. This technique recorded a false

TABLE 1 Different techniques and classifying tools of corneal status comparison

Classification methods	Accuracy
ANN ¹³	89%
Fuzzy classifier ¹³	92.94%
Neuro fuzzy classifier ¹³	92.94%
Automated neural network model ²²	80%
Segmentation of cell density ¹⁸	90%
NN ¹⁶	90%

Abbreviation: ANN, artificial neural network.

alarm rate of 0.2 per hour. Mao et al.³⁸ classified EEG datasets using a CNN. They achieved an accuracy of 74% and a loss of 0.576. Gao et al.³⁹ introduced another approach for EEG classification using a deep CNN. In a case study on CHB-MIT dataset, they obtained an accuracy of 90%.

To evaluate both time- and frequency-domain EEG signal analysis, Zhou et al.⁴⁰ worked on two distinct public databases: EEG intracranial Freiburg and scalp CHB-MIT database. The theory argues a categorization approach that does not require feature extraction. They concluded that the frequency-domain signal representation outperforms the time-domain signal representation for EEG signal analysis.

THE PROPOSED AUTOMATIC DIAGNOSIS TECHNIQUE

This paper presents a deep learning technique for AD from corneal images and EEG signals. The main contribution is to allow automated diagnosis from both corneal images and EEG signals. The proposed model is deployed on corneal images and EEG signals, separately. The deep learning model consists of several main layers. The first layer is the CNV. The second layer is the PL. Both CNV and PL layers are deployed for feature extraction. The CNV layer extracts the features from the input images by applying a set of filters, which are responsible for extracting the features. In addition, the PL layer is responsible for reducing the number of features based on pixel selection. The process of pixel selection is based on a maximum pooling technique. The maximum pooling is deployed to select the maximum value from each window in the feature map. Furthermore, a classification network performs the classification process. This network consists of an FC layer, which is responsible for transforming the generated feature map into a vector to be enrolled to the classifier. A dense layer with a Soft-max activation function is adopted in the classifier.

| Convolutional layer

The CNV layer employs a technique called linear spatial filtering on the input image. The filter is commonly referred to as a kernel. All filters are applied on the whole image.³³ This layer generates feature maps. Each map emphasizes some of the original image distinctive features.

The actual region in Figure 1, represented by the square, is filtered to form the first component of the map as per the following formula.

$$f_{\delta x, y \delta} = \sum_{i, j} a_{ij} \cdot b_{x \delta p_i, y \delta j}$$

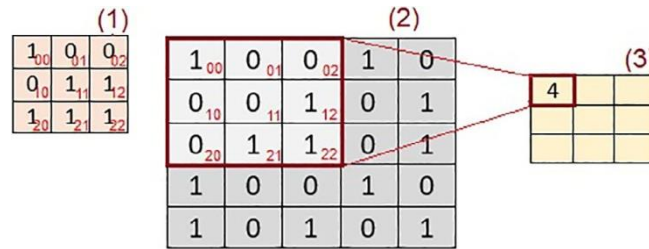


FIGURE 1 Calculation of the first component of a feature map (3), with a 3 × 3 filter applied to 5 × 5 area

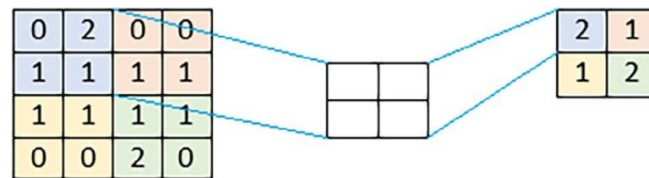


FIGURE 2 Example of maximum pooling operation

where $f(x, y)$ is the produced feature map component at location (x, y) ; a_{ij} is an element from the filter matrix, Matrix 1 in Figure 1; $b_{x+i,y+j}$ is the element from the spatial area of input data; b_{ij} elements represent the red part of Matrix 2; i, j are the row and column indices of present element pairs in the filter, and these indices are the red numbers in right bottom corners. In addition, n is the number of elements in the filter.

As shown in Figure 1, a matrix of size 5×5 , and a filter of size 3×3 are used to produce the first component of the feature map. In the convolution process, filtering is performed with a certain stride that represents the step size, which determines the relative position shifts.

| Pooling layer

This layer performs feature extraction in neural networks. It decreases the size of images or feature maps. This is accomplished by merging adjacent pixels in the spatial domain into a single value. This representative value is the maximum or the mean value of the combined pixels. The proposed technique employs maximum pooling. It produces the maximum value from a set of features in the feature map. The maximum pooling is illustrated in Figure 2.

The pooling produces smaller dimensions of features. It reduces the number of network parameters, and hence reduces the calculations and controls the overfitting. Moreover, pooling makes the network resistant to minor transformations, rotations and distortions in the source images, since the maximum/average value in a local neighborhood is taken.

| Rectified linear unit

The Rectified linear unit (ReLU) accelerates the training process by maintaining positive values and mapping negative values to zero.⁴¹ The output of the ReLU layers is obtained with the following linear activation function,

$$f(x) = \max(0, x) \tag{2}$$

Each convolution layer performs convolution on a feature map produced from the input image. Then, the ReLU is applied on each of the feature maps, separately. This is followed by the maximum pooling operation on each feature map. By combining these layers, a non-linear network is created, which reduces the feature dimensions, while keeping features equivariance to scaling and translation.

| FC layer

In the output layer of this multi-layer perceptron, a softmax activation function is used. The concept of “FC” indicates that each neuron in the preceding layer is connected to a corresponding neuron in the subsequent one.

Combining high-level features produced from convolution and pooling layers might be better for classification. These combined features need to be classified. That is what the FC layer makes based on the training dataset. In addition, it is a non-expensive way of learning such a combination of non-linear features. The Soft-max is used as an activation function in the FC layer output, where the sum of its output probabilities is 1.

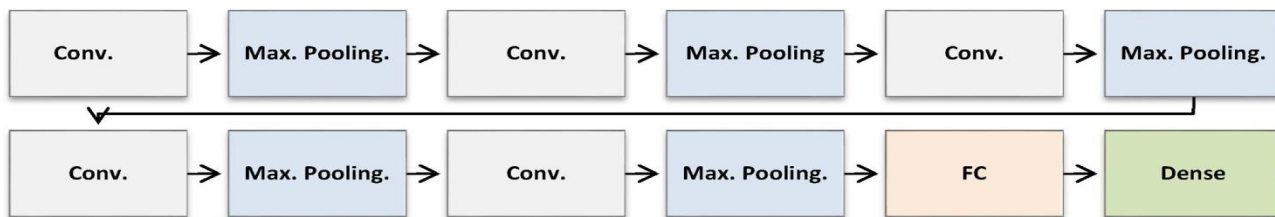


FIGURE 3 Contents of the proposed deep learning model for corneal image diagnosis

TABLE 2 Layer description pf the proposed CNN model

Utilized layer type	Shape of the output
CNV layer 1	(222, 222, 16)
Pooling layer 1	(111, 111, 16)
CNV layer 2	(109, 109, 32)
Pooling layer 2	(54, 54, 32)
CNV layer 3	(52, 52, 64)
Pooling layer 3	(26, 26, 64)
CNV layer 4	(24, 24, 128)
Pooling layer 4	(12, 12, 128)
CNV layer 5	(10, 10, 256)
Pooling layer 5	(5, 5, 256)
Global average layer	(256)
Dense layer	(2)

Abbreviations: CNN, convolutional neural network; CNV, convolutional layer.

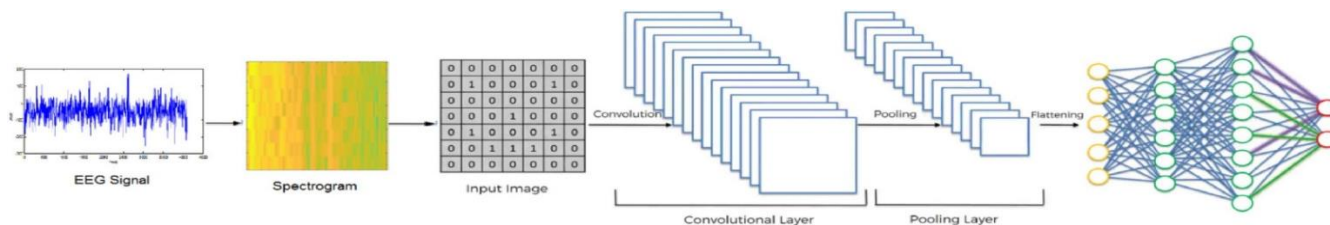


FIGURE 4 Block diagram of the proposed approach

Combining the above-mentioned layers, the convolution and pooling layers work as feature extractors, while the FC layer plays the classifier role. The Soft-max operation is shown in Equation (3).

$$P_{ij} = \frac{e^{x^T w_j}}{\sum_k e^{x^T w_k}} \tag{3}$$

k/41

| Optimization

Optimization techniques are used to minimize a cost function. The idea of an optimization technique is to bring down the error, where the cost function is very high. Therefore, the weights have to be adjusted in such a suitable way.

One of the most important optimization techniques is the gradient decent technique. In gradient descent optimization, the learning rate and the optimum value should be known, because if there is a high learning rate, the optimization would not end with convergence. If we use a very low learning rate, it might take an infinite time to get to convergence. Therefore, we need to come up with the optimum value of the learning rate. Once this is accomplished, the error function is reduced. This is similar to the end of the training process. The cost and loss functions can be calculated as follows:

$$C = \frac{1}{2} \sum (\hat{Y} - Y)^2 \tag{4}$$

$$L = \frac{1}{4} \sum_k \|X - Y\|^2 \tag{5}$$

TABLE 3 Specifications of layers

Layer type	Specifications of layer		
Input layer	Input size = 224 × 224		
Convolutional layer	No. of filters = 32	Kernel size = 3	Activation function: ReLU
Max. pooling	Pooling window size = 2 × 2		
Batch normalization			
Global average			
Dense layer	No. of classes = 8	Activation function: Softmax	

TABLE 4 Information of the utilized datasets for testing the proposed technique

Patient ID	Gender	Age	No. of seizures
Chb01	Female	11	7
Chb08	Male	3.5	5
Chb20	Female	6	8

$$rL_w = \frac{1}{4} \sum_k \|X - Y\|^2 \tag{6}$$

where C is the difference between the expected value \hat{Y} and real value Y divided by 2, L is the loss function for an image X with w parameters or weights.

| Proposed model for corneal diagnosis

The proposed model for AD from corneal images consists of five convolution and five maximum pooling layers for feature extraction. In addition, an FC layer, as shown in Figure 3, performs the classification process. Table 2 shows the proposed model with the output shape of each layer.

The proposed deep-learning-based model consists of a CNV layer, maximum pooling layers, and a global average pooling layer at the end. The dimensions of the input images are 224×224 . A CNV layer has 32 filters, followed by size 2 maximum pooling. Finally, a dense layer is used for the 2-state classification decision in the detection and the prediction framework.

| Proposed model for EEG signal diagnosis

In this case study, the objective is to introduce a deep learning model to solve the problem of epilepsy diagnosis. The common format of the input data for the deep learning model is the images. Therefore, there is a need to transform the EEG signals into images. This process is performed by generating the spectrograms of the input EEG signals. A spectrogram is a colored amplitude-dependent visual depiction of the spectrum of frequencies as they change over time. It depicts how a signal frequency changes over time. This graph shows the energy content expressed as a function of frequency on the vertical axis and time on the horizontal axis. For an EEG signal, spectrogram is considered a time evolution estimation of the frequency content of this signal.

To calculate the spectrogram, first, the EEG signal is segmented into equal-length windows, which may or may not overlap. The non-stationary nature of the EEG signal should be considered, when setting the window size. The fundamental concept is to show the spectral features of a non-stationary EEG signal as a sequence of spectral pictures. The segment length for a typical non-stationary signal should be small enough, such that the frequency variation is not noticeable. After that, we compute the short-time Fourier transform. Finally, we display each power spectrum. These spectra are computed segment by segment, and stacked side by side to compose a colored map that is magnitude-dependent.

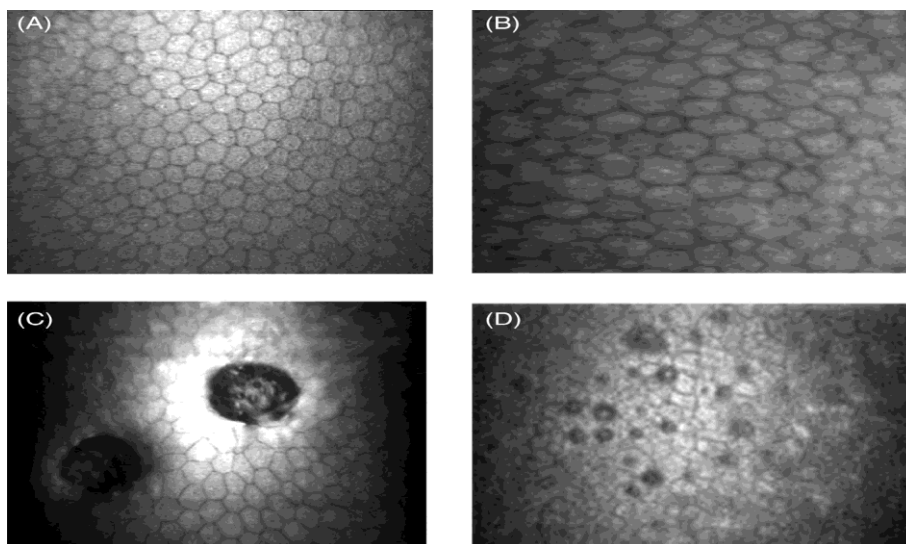


FIGURE 5 Corneal image samples from the used dataset, (A) and (B) are normal images and (C) and (D) are abnormal images

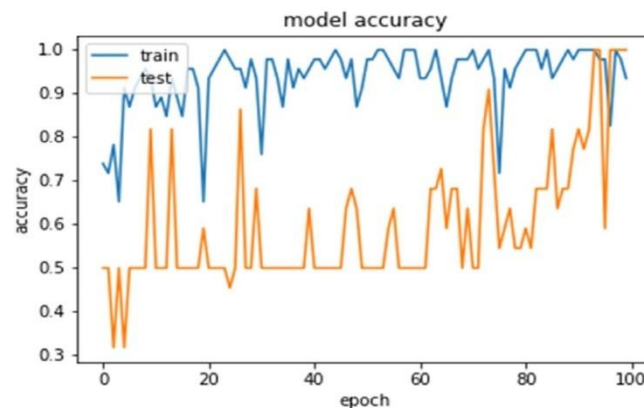


FIGURE 6 Accuracy of the proposed deep learning model

The proposed deep-learning-based model can be used for both detection, and prediction. The proposed model consists of a CNV layer, maximum pooling layers, and a global average pooling layer at the end. Figure 4 shows the block diagram of the proposed model. Images used as input are of size 224×224 . The CNV layer has 32 filters, followed by a size-2 maximum pooling. Finally, a size-3 dense layer is used. The size-3 dense layer is used for the 3-state classification, while for the 2-state classification as in the detection and prediction processes, a size-2 dense layer is used. Layer specifications are shown in Table 3.

Simple training is possible due to the designed three-layer structure of the CNN. Moreover, this scenario increases the potential of the online clinical diagnosis of epilepsy activities. The proposed technique was tested on three patients. Seventy percent of the data is used for training, and the remaining 30% is used for testing and validation. In

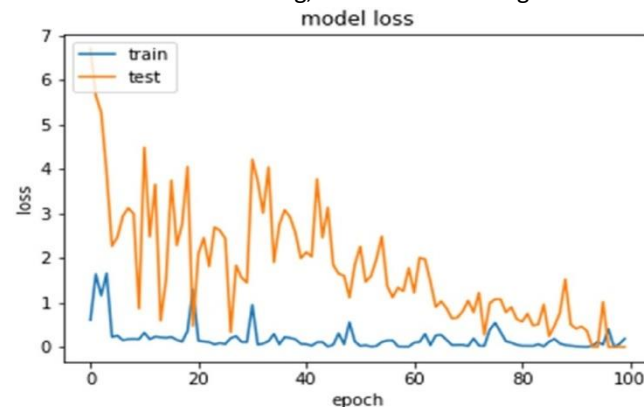


FIGURE 7 Loss of the proposed deep learning model

3-state classification, 90 images have been used in experiments, and classified into three main categories. Sixty three images have been used for training, and 27 images have been used for testing. On the other hand, 60 images have been used in experiments for 2-state classification, 42 images for the training phase, and 18 images for the testing phase.

2 | SPECIFICATIONS OF THE UTILIZED DATASET

This section is devoted to describing the used dataset specifications. The dataset of the EEG signals has been taken from the Massachusetts Institute of Technology in the United States (CHB-MIT). This dataset is available through the website, <http://physionet.org/physiobank/database/chbmit/>. The recorded data have been collected for 23 children using scalp electrodes, with a sampling frequency of 256 Hz. The ictal state is defined as the period taken by the patients to experience the seizure onset, while the inter-ictal period is the between-seizure normal state. The pre-ictal period is defined as the transition between the two previous periods. Table 4 gives the investigated three patients' infor-

mation: chb01, chb08, and chb20. Each of these patients has a different number of seizures. On the other hand, the corneal dataset is available through the website, <http://bioimlab.dei.unipd.it/Endo%20Aliza%20Data%20Set.htm>. The normal and abnormal samples of corneal images are shown in Figure 5.

3 | RESULTS OF THE COMPUTER SIMULATION EXPERIMENTS

This section presents the different simulation experiments, which have been performed for evaluating the performance and accuracy of the automatic diagnosis technique. The accuracy of the presented technique measures the traditional CNN model robustness. It can be calculated by Equation (7):

$$\text{Accuracy} = \frac{\text{No: of images that were accurately classified}}{\text{Total No: of images}} \times 100 \quad (7)$$

| Results of the corneal image classification experiment

The results of the corneal image classification experiment are presented in this section. As previously described, the presented technique contains different layers as shown in Figure 3. The accuracy and loss of the training stage of the deep learning model are given in Figures 6 and 7. From these figures, it is clear that the accuracy of the proposed technique reaches 100% and the loss is close to zero. The proposed technique results are compared with those of the related research works and the other utilized techniques.

TABLE 5 Accuracy results for patient 1

Channels	FP1-F7	F7-T7	T7-P7	P7-O1	FP1-F3	F3-C3	C3-P3	P3-O1	FP2-F4	F4-C4	C4-P4	P4-O2	FP2-F8	F8-T8	T8-P8	P8-O2	FZ-CZ	CZ-PZ	P7-T7	T7-FT9	FT9-FT10	FT10-T8	T8-P8
CH 01	01	02	03	04	05	06	07	08	09	10	11	12	13	14	15	16	17	18	19	20	21	22	23
Three-state classification accuracy (%)	70.37	48.15	62.96	55.56	37.04	62.96	48.15	55.56	62.96	59.26	74.07	62.96	40.74	62.96	51.85	44.44	59.26	40.74	44.44	51.85	48.15	51.85	51.85
Detection accuracy (%)	61.11	72.22	83.33	72.22	77.78	83.33	61.11	77.78	83.33	77.78	94.44	77.78	50.00	55.56	72.22	66.67	83.33	72.22	83.33	72.22	77.78	55.56	66.67
Prediction accuracy (%)	66.67	66.67	83.33	61.11	66.67	94.44	77.78	61.11	88.89	83.33	83.33	55.56	50.00	83.33	77.78	66.67	77.78	61.11	83.33	50.00	61.11	77.78	77.78

TABLE 6 Accuracy results for patient 8

Channels	FP1-F7	F7-T7	T7-P7	P7-O1	FP1-F3	F3-C3	C3-P3	P3-O1	FP2-F4	F4-C4	C4-P4	P4-O2	FP2-F8	F8-T8	T8-P8	P8-O2	FZ-CZ	CZ-PZ	P7-T7	T7-FT9	FT9-FT10	FT10-T8	T8-P8
CH 08	01	02	03	04	05	06	07	08	09	10	11	12	13	14	15	16	17	18	19	20	21	22	23
Three-state classification accuracy (%)	48.15	40.74	59.26	51.85	44.44	25.93	37.04	44.44	37.04	44.44	48.15	51.85	48.15	51.85	62.96	48.15	48.15	33.33	66.67	48.15	44.44	51.85	70.37
Detection accuracy (%)	50.00	33.33	55.56	55.56	22.22	50.00	50.00	61.11	55.56	50.00	66.67	55.56	50.00	38.89	72.22	50.00	66.67	50.00	50.00	50.00	33.33	44.44	66.67
Prediction accuracy (%)	66.67	72.22	88.89	66.67	83.33	66.67	50.00	61.11	66.67	55.56	50.00	61.11	61.11	77.78	66.67	55.56	61.11	38.89	83.33	77.78	55.56	66.67	77.78

TABLE 7 Accuracy results for patient 20

Channels	FP1-F7	F7-T7	T7-P7	P7-O1	FP1-F3	F3-C3	C3-P3	P3-O1	FZ-CZ	CZ-PZ	FP2-F4	F4-C4	C4-P4	P4-O2	FP2-F8	F8-T8	T8-P8	P8-O2	P7-T7	T7-FT9	FT9-FT10	FT10-T8	T8-P8
CH 20	01	02	03	04	06	07	08	09	11	12	14	15	16	17	19	20	21	22	24	25	26	27	28
Three-state classification accuracy (%)	51.85	66.67	66.67	55.56	62.96	51.85	62.96	70.37	48.15	51.85	55.56	51.85	62.96	55.56	51.85	55.56	59.26	59.26	55.56	51.85	55.56	55.56	55.56
Detection accuracy (%)	50.00	66.67	77.78	55.56	38.89	33.33	61.11	50.00	61.11	66.67	38.89	50.00	61.11	55.56	66.67	66.67	66.67	61.11	66.67	61.11	72.22	66.67	61.11
Prediction accuracy (%)	94.44	88.89	100.00	94.44	94.44	83.33	83.33	94.44	55.56	66.67	94.44	94.44	83.33	100.00	77.78	94.44	100.00	100.00	100.00	72.22	66.67	77.78	100.00

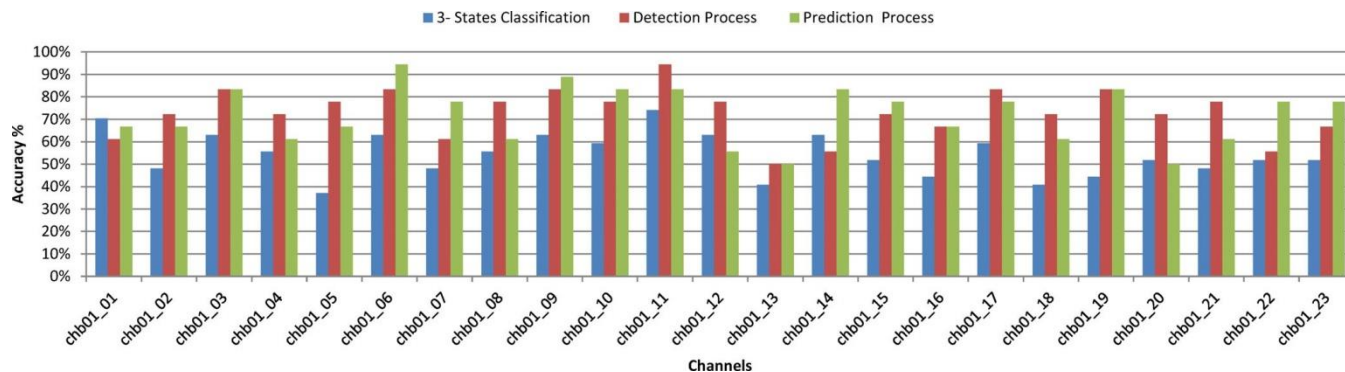


FIGURE 8 Accuracy results for patient 1

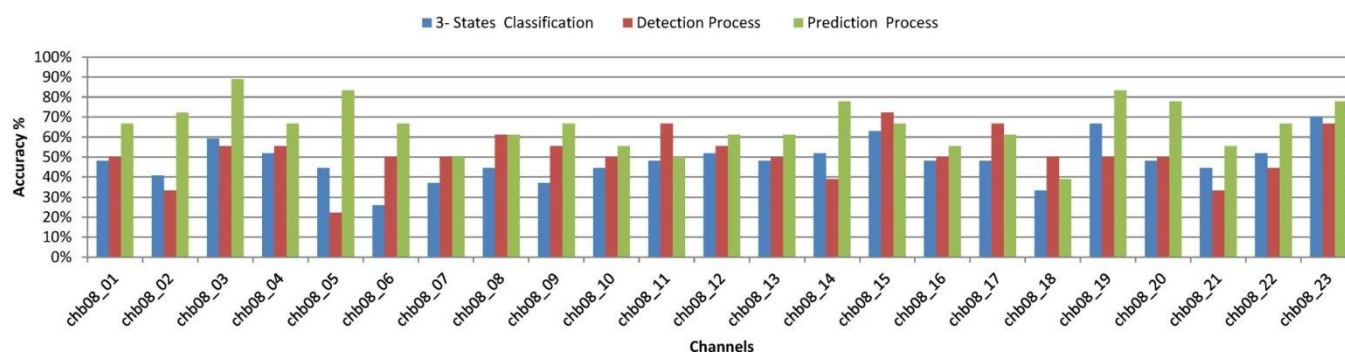


FIGURE 9 Accuracy results for patient 8

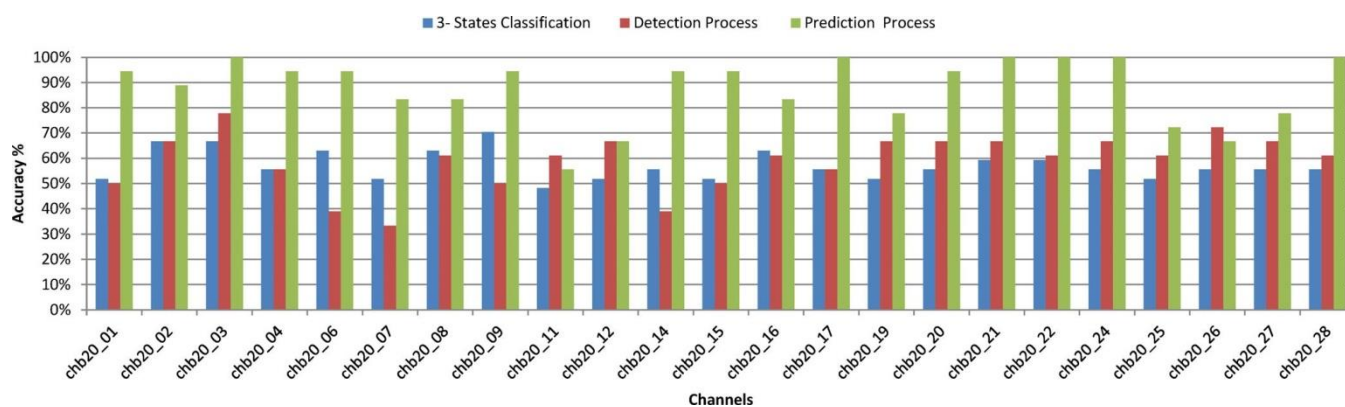


FIGURE 10 Accuracy results for patient 2

| Results of EEG signal classification experiments

The experimental results of the EEG signal classification are presented in this section. The proposed EEG signals classification technique has four different layers, which are the CNV, maximum pooling, dense, and softmax layers. Tensorflow and Keras have been used for obtaining the simulation results.

The proposed EEG signal classification methodology has been evaluated on time-domain signals from the CHB-MIT databases. The proposed classification model has been tested through three scenarios. Two types of experiments on two-state and three-state classification scenarios have been considered. In the two-state scenario, both normal versus

TABLE 8 Comparison between the proposed and Zhou's CNN technique

Patient ID	Detection		Prediction	
	Proposed	Zhou ⁴ ₀	Proposed	Zhou ⁴⁰
1	94.44	99.3	94.44	90.5
8	72.22	54.8	88.89	50.88
20	77.78	49.0	100.00	59.0

Abbreviation: CNN, convolutional neural network.

pre-ictal, and normal versus ictal cases are considered. Another scenario has been considered for the three-state classification problem, which is the normal versus seizure versus pre-ictal. The proposed model has been tested on all the 23 channels for the three patients. After the spectrogram calculation, the classification accuracy results for all different 23 channels for the three patients have been analyzed and the accuracy values are tabulated in Tables 5–7 and Figures 8–10.

Patient No. 1 has seven epileptic seizures. Table 5 tabulates the accuracy of EEG signal classification on the 23 channels. In the three-state scenario and the detection process, it is noticed that the best classification results are given by channel 11. The accuracy of this classification case is between 74.07% and 94.44%. In the prediction case, the best classification result is given by channel 06, and the accuracy is 94.44%.

Patient No. 8 has five epileptic seizures. The results of this experiment using the same simulation scenarios utilized for Patient No. 1 are tabulated in Table 6. The accuracy of the three-state classification is 70.37% from channel 23. In the detection process, the best classification is given from channel 15, where the accuracy is 72.22%. In the prediction process, the highest accuracy is 88.89% from channel 03.

The last classification experiment has been performed on Patient No. 20, who has 8 seizures. The results are tabulated in Table 7. From these results, in the three-state classification case, the highest accuracy from channel 09 equals 70.37%. In the detection process, the classification accuracy equals 77.68% from channel 03. In the prediction process, the highest accuracy equals 94.44% from seven channels, as shown in Table 7 and Figure 10.

Finally, to emphasize the superiority of the proposed technique, a comparison between the proposed technique and Zhou CNN⁴¹ is presented in Table 8. The comparison is performed from the accuracy perspective. This comparison confirms the superiority of the proposed model in the detection and prediction processes.

CONCLUSION

The automatic diagnosis based on inspection of medical images and signals is considered an attractive research field. In this research paper, medical signal processing has been employed to design a simple and efficient automated diagnosis tool from signals and images. An efficient AD technique using a CNN algorithm for EEG signal and corneal image classification has been proposed. The proposed technique has been tested and validated on different database. The simulation results reveal that the proposed technique achieves high accuracy in both seizure detection and prediction. In addition, the detection of anomalies from corneal images has been implemented with high accuracy levels. This work can be an effective step for building complete and efficient automated diagnosis systems.

ACKNOWLEDGMENT

Princess Nourah bint Abdulrahman University Researchers Supporting Project number (PNURSP2022R66), Princess Nourah bint Abdulrahman University, Riyadh, Saudi Arabia.

REFERENCES

- Balasubramian M, Louise A, Roger W. Fractal dimension based corneal fungal diagnosis. *Proc SPIE*. 2006;6312:200-211.
- Fabijan A. Corneal endothelium image segmentation using feedforward neural network: Proceedings of the Federated Conference on Computer Science and Information Systems; IEEE Catalogue Number, 2017:629-637.
- Bucht CPer S, Göran M. "Fully automated corneal endothelial morphometric of images captured by clinical specular microscopy". Oph-

- thalmic Technologies XIX. International Society for Optics and Photonics; 2009;7163:125-136.
4. Tang M, Shekhar R, Huang D. Curvature mapping for detection of corneal shape abnormality. *IEEE Trans Med Imaging*. 2005;24(3): 16-25.
 5. Girisha V, Chandra KV. Machine intelligence on confocal microscope for detection of endothelium layer of corneal disease: Proceedings of IJCTER; 2016:148-211.
 6. Rezaadeh IM, Maghooli K. Investigating and validation numerical measures of corneal topographic data is Lasik surgery outcome using wavelet transform: Proceedings of IEEE; 2006:153-159.
 7. Ayala G, Diaz M, Martinez-Costa L. Granulometric moments and corneal endothelium status. *Pattern Recognit*. 2001;34:1219-1222.
 8. Nadachi R. Automated corneal endothelial cell analysis in fifth annual. Paper presented at: IEEE Symposium on Computer Based Medical Systems; 1992:14-17.
 9. Sanchez F. Automatic segmentation of contours of corneal cells. *Comput Biol Med*. 1999;29:243-155.
 10. Mahzoun M, Okazaki K, Kawai H, Sato Y, Tamura S, Kani K. Detection and complement of hexagonal borders in corneal endothelial cell image. *Med Imaging Technol*. 1996;14(1):56-65.
 11. Habrat K, Habrat M. Cell detection in corneal endothelial images using directional filters. *Image Processing and Communications Challenges*; 389. Springer; 2016:113-123. https://doi.org/10.1007/978-3-319-23814-2_14
 12. Piorkowski A, Nurzynska K, Gronkowska-Serafin J, Selig B, Boldak C, Reska D. Influence of applied corneal endothelium image segmentation techniques on the clinical parameters. *Comp Med Imag Grap*. 2017;55:13-27.
 13. Acharya UR. Computer-based classification of eye diseases: Proceedings of the 28th IEEE EMBS Annual International Conference, New York City, 30 August-3 September 2006.
 14. Habrat M, Piorkowski A. Cell detection in corneal endothelial images using directional filters. *Image Processing and Communications Challenges 7*; Springer; 2016:113-123.
 15. Alferdo Ruggeri And Enrico Grisan “A new system for the automatic estimation of endothelial cell density in donor corneas”, *Br J Ophthalmol*, 306–311, 2005, 89.
 16. Foracchia M, Ruggeri A. Estimating cell density in corneal endothelium by means of Fourier analysis: Proceedings of IEEE; 2002:23-26.
 17. Gavet Y. Visual perception based automatic recognition of cell mosaics in human corneal endothelium microscopy images. *Image Anal Stereol*. 2008;27(1):53-62.
 18. Grisan E, Paviotti A. A lattice estimation approach for the automatic evaluation of corneal endothelium density: Proceedings of IEEE; 2005:150-168.
 19. Griffiths GW. Analysis of cornea curvature using radial basis functions-Part 1-methadology. *Comput Biol Med*. 2016;77:272-284. <https://doi.org/10.1016/j.combiomed.2016.08.011>.
 20. Klyce D. Computer assisted corneal topography. *Invest Ophthalmol Vis Sci*. 1984;25(12):210-230.
 21. Fabijanska A. Automatic segmentation of corneal endothelial cells from microscopy images. *Biomed Signal Process Control*. 2019;47:145-158.
 22. Cun L, Bottou Y. Gradient-based learning applied to document recognition: Proceedings of the IEEE; 2008:482-456.
 23. Ranzato M, Huang FJ, Boureau Y, LeCun Y. Unsupervised learning of invariant feature hierarchies with applications to object recognition. *IEEE Comput Vis Pattern Recognit*. 2007;1-8. doi:10.1109/CVPR.2007.383157.
 24. Srivastava N, Hinton G, Krizhevsky A, Sutskever I, Salakhutdinov R. Dropout: a simple way to prevent neural networks from over fitting. *J Mach Learn Res*. 2014;15:1929-1958.
 25. Fisher RS, Acevedo C, Arzimanoglou A, et al. ILAE official report: a practical clinical definition of epilepsy. *Epilepsia*. 2014;55(4):475-482.
 26. WHO, <http://www.who.int/en/news-room/fact-sheets/detail/epilepsy>. Accessed June 16, 2020.
 27. Schomer D, Lopes da Silva F, *Niedermeyer's Electroencephalography: Basic Principles, Clinical Applications, and Related Fields*, Oxford University Press; 2017.
 28. Abou-Khalil B, Musilus KE, eds. *Atlas of EEG & Seizure Semiology*. Elsevier; 2006.
 29. Dalton A, Patel S, Chowdhury AR, et al. Development of a body sensor network to detect motor patterns of epileptic seizures. *IEEE Trans Biomed Eng*. 2012;59(11):3204-3211.
 30. Khamis H, Mohamed A, Simpson S. Frequency–moment signatures: a method for automated seizure detection from scalp EEG. *Clin Neurophysiol*. 2013;124(12):2317-2327.
 31. Zhou W, Liu Y, Yuan Q, Li X. Epileptic seizure detection using lacunarity and Bayesian linear discriminant analysis in intracranial EEG. *IEEE Trans Biomed Eng*. 2013;60(12):3375-3381.
 32. Meier R, Dittrich H, Schulze-Bonhage A, Aertsen A. Detecting epileptic seizures in long-term human EEG: a new approach to automatic online and real-time detection and classification of polymorphic seizure patterns. *Journal of Clinical Neurophysiology*. 2008;25(3): 119-131.
 33. Vidyaratne L, Glandon A, Mahbulul A, Iftekharuddin M. Deep recurrent neural network for seizure detection. *International Joint Conference on Neural Networks (IJCNN)*. IEEE; 2016:1202-1207.

34. Shoeb AH & Gutttag JV Application of machine learning to epileptic seizure detection: Proceedings of the 27th International Conference on Machine Learning (ICML-10); 2010:975-982.
35. Pramod S, Page A, Mohsenin T, Oates T. Detecting epileptic seizures from eeg data using neural networks. *arXiv Preprint arXiv: 1412.6502*, 2014.
36. Turner J, Page A, Mohsenin T, Oates T. Deep belief networks used on high resolution multichannel electroencephalography data for seizure detection. *Big Data Becomes Personal: Knowledge into Meaning*; Papers from the AAAI Spring Symposium Association for the Advancement of Artificial Intelligence; 2014.
37. Emami A, Kunii N, Matsuo T, Shinozaki T, Kawai K, Takahashi H. Seizure detection by convolutional neural network-based analysis of scalp electroencephalography plot images. *NeuroImage Clin.* 2019;22:101684.
38. Mao W-I, Fathurrahman H, Lee Y, Chang T-W. EEG dataset classification using CNN method. *J Phys Conf Ser.* 2020;1456:012017. <https://doi.org/10.1088/1742-6596/1456/1/012017>
39. Gao Y, Gao B, Qiang C, Jia L, Yingchun Z. Deep convolutional neural network-based epileptic electroencephalogram (EEG) signal classification. *Front Neurol.* 2020;11:375. <https://doi.org/10.3389/fneur.2020.00375>
40. Zhou M, Tian C, Cao R, et al. Epileptic seizure detection based on EEG signals and CNN. *Front Neuroinform.* 2018;12:95.
41. Sannino G, De Pietro G. A deep learning approach for ECG-based heartbeat classification for arrhythmia detection. *Future Gener Comput Syst.* 2018;86:455. <https://doi.org/10.1016/j.future.2018.03.057>